

Mid-Infrared Optical Absorption in Undoped Lamellar Copper Oxides

J. D. Perkins, J. M. Graybeal, M. A. Kastner, R. J. Birgeneau, J. P. Falck, and M. Greven
*Center for Material Science and Engineering and Department of Physics, Massachusetts Institute of Technology,
 Cambridge, Massachusetts 02139*

(Received 11 March 1993; revised manuscript received 21 June 1993)

Common optical absorption features are observed near 0.5 eV in four undoped single-crystal copper oxides: La_2CuO_4 , Nd_2CuO_4 , Pr_2CuO_4 , and $\text{Sr}_2\text{CuO}_2\text{Cl}_2$. These absorption bands are shown to be weakly electric dipole allowed excitations of the CuO_2 layers. The features are ascribed to an exciton near 0.4 eV, probably of crystal-field origin, with strong multimagnon sidebands. Our observations provide an important basis for understanding the doped materials.

PACS numbers: 74.25.Gz, 71.70.-d, 74.62.Dh, 74.72.Jt

The mid-infrared optical properties of the doped lamellar copper oxides have been the subject of intense interest [1-3] since the discovery of high temperature superconductivity. A broad absorption band peaked near 0.5 eV is observed together with additional absorption in the vicinity of 1.5 eV. While much speculation has appeared, the absence of sharp spectral features has made a definitive interpretation of these excitations very difficult. Surprisingly, less attention has been paid to the mid-infrared spectra in the undoped materials.

In this Letter we report the observation of clearly resolved optical excitations centered near ~ 0.5 eV in a series of undoped single-crystal copper oxides. Similar spectra are observed in four different materials, appearing only for the electric field polarized parallel to the CuO_2 planes. This universality demonstrates that the absorption bands result from intrinsic excitations of the CuO_2 layers. Associated with a sharp peak near 0.4 eV are strong multimagnon sidebands, whose characteristic features are in accord with measured magnon energies. Although the precise origin of the sharp peak is not fully resolved, the simplest interpretation is that it arises from transitions involving the $d_{x^2-y^2}$ and $d_{3z^2-r^2}$ crystal field levels of the Cu ions. A second band near 1.5 eV may originate from the $d_{x^2-y^2} \rightarrow d_{xy}$ transition. The elucidation of these issues will likely form a basis for understanding the corresponding behavior in the doped materials.

Our experiments were performed on a series of high-quality single crystals of undoped antiferromagnetic La_2CuO_4 , Nd_2CuO_4 , Pr_2CuO_4 , and $\text{Sr}_2\text{CuO}_2\text{Cl}_2$. La-, Nd-, and Pr_2CuO_4 crystals were grown by top-seeded-solution growth in Pt crucibles using CuO flux [4]. Additional La_2CuO_4 crystals were grown by the floating-zone technique, and thus were free of Pt. All La_2CuO_4 crystals were vacuum annealed to eliminate excess holes from the CuO_2 layers [5]. Before measurement, the La-, Nd-, and Pr_2CuO_4 crystals were etched in 1% Br in isopropanol to remove any surface damage or contamination. The $\text{Sr}_2\text{CuO}_2\text{Cl}_2$ crystals, grown by cooling the stoichiometric melt [6,7], were cleaved, leaving smooth clean surfaces. $\text{Sr}_2\text{CuO}_2\text{Cl}_2$ is stoichiometric as grown, and

cannot be readily doped.

The four materials share two-dimensional approximately square-planar CuO_2 layers, with comparable nearest-neighbor exchange interactions [6-8]. However, the out-of-plane structures have important differences. At high temperature, La_2CuO_4 and $\text{Sr}_2\text{CuO}_2\text{Cl}_2$ are tetragonal structures (T phase) with octahedrally coordinated Cu sites. Below ~ 530 K, La_2CuO_4 acquires a slight orthorhombic distortion. In tetragonal $\text{Sr}_2\text{CuO}_2\text{Cl}_2$, the La is replaced by Sr and the apical O by Cl. Nd- and Pr_2CuO_4 are tetragonal (T' phase) with square-planar coordinated Cu sites and no apical ions.

Optical transmission spectra were obtained in the photon energy range 0.1 to 2 eV. All four materials were examined in α polarization (electric field $\mathbf{E} \parallel \text{CuO}_2$ layer and wave vector $\mathbf{k} \perp \text{layer}$). Additional La_2CuO_4 samples were polished perpendicular to the layers for measurements with \mathbf{k} in the plane for both σ ($\mathbf{E} \parallel \text{layer}$) and π ($\mathbf{E} \perp \text{layer}$) polarizations. The sample thickness (~ 10 - $200 \mu\text{m}$) was determined both directly and from observed interference fringes using an optical dielectric constant of $\epsilon=5$ for the oxides, while we measure $\epsilon=3.6 \pm 0.4$ for $\text{Sr}_2\text{CuO}_2\text{Cl}_2$. This facilitated the measurements of quantitative absorption coefficients.

Figure 1 shows the absorption coefficients for the four materials in α polarization as a function of photon energy, measured at 10 K. Common absorption features are seen in the range 0.2 to 0.6 eV. The absorption coefficient is weak, roughly 10^3 times smaller than in heavily doped samples, and independent of photon flux. The features below ~ 0.15 eV are associated with optic phonons. The additional narrow lines which complicate the Nd- and Pr_2CuO_4 spectra correspond to intra- f -shell transitions [9], which are electric-dipole allowed as the rare-earth sites do not possess inversion symmetry. Figure 2 shows that identical La_2CuO_4 spectra are obtained in α and σ polarization; the linear background attenuation is subtracted to display the results more clearly. In π polarization the features are essentially absent. Thus the absorption bands only appear when the electric field vector lies in the CuO_2 layer.

For all four compounds, the spectra display a sharp

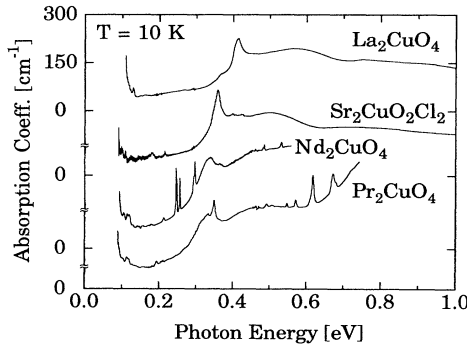


FIG. 1. Absorption coefficient vs photon energy in α polarization for La_2CuO_4 , $\text{Sr}_2\text{CuO}_2\text{Cl}_2$, Nd_2CuO_4 , and Pr_2CuO_4 . Note left axis offsets, and intra- f -shell transitions in Nd- and Pr_2CuO_4 .

low-energy line centered near 0.4 eV and a set of broader bands which extend to higher energies. The respective spectral weights of these peaks are closely similar for all measured crystals. In particular, identical results are obtained for both floating-zone and top-seeded-solution grown La_2CuO_4 crystals (Fig. 2). We display the La_2CuO_4 and $\text{Sr}_2\text{CuO}_2\text{Cl}_2$ results in more detail in Fig. 3, as they are free of the complicating intra- f -shell absorptions. In addition to the broad sidebands for $\text{Sr}_2\text{CuO}_2\text{Cl}_2$ one also observes two small lines just above the 0.35 eV peak. The La_2CuO_4 there is a shoulder on the low-energy side of the 0.4 eV peak.

The universality in the intensity and spectrum of the absorption features (Fig. 1) and the polarization dependence seen in the La_2CuO_4 crystals (Fig. 2) show that these transitions are weakly electric-dipole-allowed excitations of the CuO_2 planes. As the impurity species and concentration, although low, clearly vary between the measured samples, the observed sample-to-sample uniformity indicates that these excitations must be intrinsic. As we now show, the data provide severe constraints on the

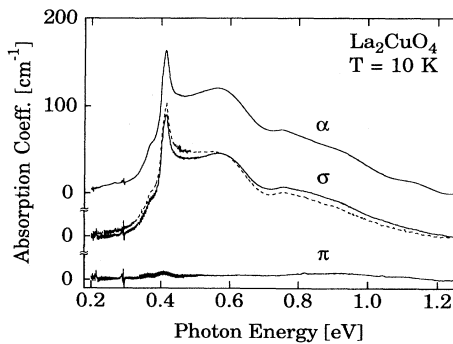


FIG. 2. La_2CuO_4 absorption coefficient vs photon energy for α , σ , and π polarizations, after subtracting the linear background. Additional σ trace (dashed line) is for a floating-zone grown crystal. Note the low-energy interference fringes.

origin of these absorptions. We shall argue that the low-energy peak is associated with a Frenkel exciton, most likely arising from transitions between the crystal-field levels of the Cu ions. We begin this argument by first discussing the sidebands.

Since all the materials correspond to $2\text{D } S = \frac{1}{2}$ Heisenberg antiferromagnets it is natural to assume that the broad features result from exciton-magnon absorption processes as discussed, for example, by Tanabe *et al.* [10] and Parkinson and Loudon [11]. Tanabe *et al.* have shown that a kind of off-diagonal exchange can generate weakly electric-dipole-allowed exciton-magnon transitions. Specifically, the effective electric dipole operator is

$$P_{\text{eff}}(\phi_{a'} \leftarrow \phi_a) = \Pi_{a'a,b} (S_{a'a} \cdot S_b) \quad (1)$$

for an ion pair a - b on different sublattices where

$$S_{a'a} = \sum_{mm'} c_{a'm}^* c_{am} \langle m' | \mathbf{S} | m \rangle$$

and c_{am} is the annihilation operator of the electron in the orbital ϕ_a with spin m . Classically, the spin-flip term involving $(S_{a'a}^+ S_b^- + S_{a'a}^- S_b^+)$ creates an exciton-magnon pair. Quantum effects will also make allowed exciton-3-magnon processes via this term. For classical spins, the diagonal term involving $S_{a'a}^z S_b^z$ does not produce exciton-magnon absorption at $T=0$ K. However, as discussed by Cowley *et al.* [12] for analogous processes in neutron scattering, for quantum spins the $S_{a'a}^z S_b^z$ terms in Eq. (1)

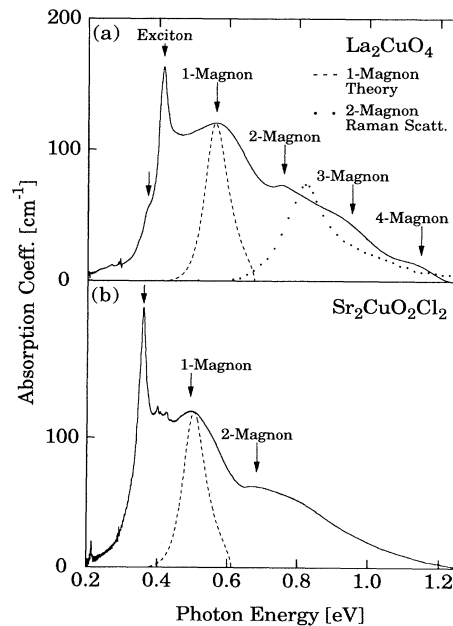


FIG. 3. La_2CuO_4 and $\text{Sr}_2\text{CuO}_2\text{Cl}_2$ absorption coefficients in α polarization. Characteristic energies for magnon sidebands are noted (see text). The predicted functional form [11] for a 1-magnon sideband (dashed line), and measured 2-magnon Raman data of Lyons *et al.* [13] (dotted line) are also shown.

will generate exciton-2-magnon and exciton-4-magnon absorption processes. Furthermore, since $|2\langle S_z \rangle|^2 \sim 0.36$ in a 2D spin- $\frac{1}{2}$ antiferromagnet at $T=0$ K, the amplitude of the 2- and 4-magnon processes should be about $\frac{1}{3}$ of that for the spin-flip 1- and 3-magnon processes. Such effects appear not to have been considered previously in the literature.

A simple Ising cluster calculation shows that the n -magnon sidebands should be located at $\sim \frac{1}{2}n(3J+J')$, where J is the ground state $d_{x^2-y^2}-d_{x^2-y^2}$ exchange and J' is the exchange in the excited state. For crystal-field excitons we expect a substantially reduced J' from overlap considerations alone; $J'=J/6$ for the $d_{3z^2-r^2}$ exciton and $J'=0$ for the d_{xy} and $d_{xz,yz}$. For simplicity we set $J'=0$. This simple model predicts that the 1-magnon peak should occur ~ 0.19 eV above the exciton line. The measured offset from the peak at 0.41 eV (0.36 eV) is 0.15 eV (0.14 eV) for La_2CuO_4 ($\text{Sr}_2\text{CuO}_2\text{Cl}_2$). We show in Fig. 3 the predicted positions for the 2-, 3-, and 4-magnon peaks relative to the 1-magnon peak assuming a constant energy difference of $3J/2 \approx 0.19$ eV. Clearly the predicted 2-magnon position agrees well with the observed second peak in both La_2CuO_4 and $\text{Sr}_2\text{CuO}_2\text{Cl}_2$. In the orthorhombic La_2CuO_4 absorption there are also pronounced shoulders at the predicted 3- and 4-magnon positions although these features are not evident in the $\text{Sr}_2\text{CuO}_2\text{Cl}_2$ data.

To explain the full spectra, a proper calculation for the exciton-multimagnon absorption in quantum spin systems must be carried out; unfortunately, no such theory exists. We show in Fig. 3 the prediction of Parkinson [11] for the exciton-1-magnon absorption spectrum for classical spins, using $J'=0$ and assuming that the narrow ~ 0.4 eV peak is the exciton. This classical theory predicts the peak position well but underestimates the peak width. Currently no theory exists for the 2- and 4-magnon sidebands. The 2-magnon sideband should be similar, albeit not identical, to the spectrum observed with 2-magnon Raman scattering. We show in Fig. 3 the Raman spectrum of La_2CuO_4 [13] with the zero of energy taken at the 0.41 eV peak. As expected, there is a discrepancy in the 2-magnon peak position since the Raman spectrum does not include exciton-magnon interactions. Nevertheless, their overall shapes are similar. Our crude estimate of $\frac{1}{3}$ for the relative intensities of the 1- and 2-magnon processes also seems reasonable. Therefore, we conclude that the absorption from above the exciton line to ~ 1.2 eV is well accounted for by exciton-multimagnon absorption processes. Additional peaks just above the primary line in $\text{Sr}_2\text{CuO}_2\text{Cl}_2$ (Fig. 3) have energies close to known optic phonons in $\text{Sr}_2\text{CuO}_2\text{Cl}_2$, which have the requisite E_u symmetry [14]. These peaks may correspond to phonon sidebands.

Not only the energy, but also the intensity of the magnon sidebands agrees with expectations. Examination of the matrix elements in Eq. (1) (see Ref. [10]) shows that

the integrated strength of the sideband should scale roughly as the square of the exchange energy, hence as the square of its energy shift. For crystal-field excitons in RbMnF_3 , for example, the shift of the magnon sideband is ~ 80 cm^{-1} and the integrated strength is ~ 1000 cm^{-2} [15]. For the copper oxides our measured shift is ~ 1500 cm^{-1} , from which the scaling argument predicts a strength of $\sim 4 \times 10^5$ cm^{-2} . The observed strength is 10^6 cm^{-2} . There is great uncertainty in this comparison because of the difference in crystal structures, in the states involved in the exciton for the two materials, and in the width of the sidebands in the Cu oxides. Nonetheless, the observation that the strength is of the expected magnitude is consistent with the idea that the magnon sideband, and by implication the exciton itself, is an intrinsic excitation of the CuO_2 layer.

While identification of the sidebands seems unambiguous, the origin of the 0.4 eV peak is more difficult to ascertain. Although close to the requisite energy for 2-magnon creation, we know of no mechanism which generates direct 2-magnon electric-dipole absorption in the tetragonal crystals. Further, such an idea for the main line would leave the sidebands unexplained. The low-energy dipole-allowed exciton is expected to result from charge transfer (CT) of electrons from O to Cu. However, the CT excitation of separated electrons and holes has an energy ~ 2 eV [5], and we know of no theory that predicts such a large binding energy (~ 1.6 eV) for CT excitons. We therefore consider the possible crystal-field excitons.

Point ion calculations predict that the $d_{x^2-y^2} \rightarrow d_{xy}$ transition is lowest in energy. However, the d_{xy} state is coupled to the $d_{x^2-y^2}$ by the orbital angular momentum operator L_z . If it were just 0.4 eV above the $d_{x^2-y^2}$, the d_{xy} state would, through spin-orbit coupling, give rise to extremely large anisotropies in the g value, and thereby the spin susceptibility and the anisotropic exchange, as well as a large and anisotropic Van Vleck susceptibility. None of these are observed thus ruling out this identification. Figure 4 shows that there is another ab-

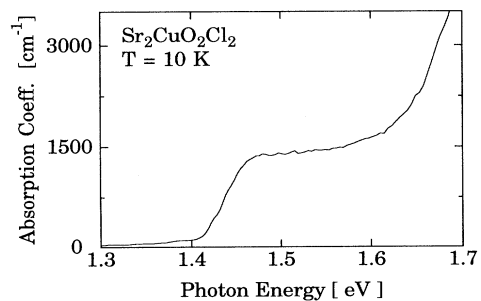


FIG. 4. Strong ~ 1.5 eV absorption band observed in $\text{Sr}_2\text{CuO}_2\text{Cl}_2$ at 10 K, identified as arising from a $d_{x^2-y^2} \rightarrow d_{xy}$ exciton. The charge-transfer absorption edge begins at 1.65 eV.

sorption band at ~ 1.5 eV in $\text{Sr}_2\text{CuO}_2\text{Cl}_2$. Electroreflectance [16] in La_2CuO_4 and Raman data [17] in Gd_2CuO_4 and other oxides indicate a similar feature at ~ 1.5 eV with the symmetry of the $d_{x^2-y^2} \rightarrow d_{xy}$ transition. Thus the d_{xy} state is naturally located at ~ 1.5 eV. The absorption coefficient for this band is so large that we can only observe it in $\text{Sr}_2\text{CuO}_2\text{Cl}_2$, which can be cleaved to ~ 10 μm thickness.

Point ion calculations predict the $d_{x^2-y^2} \rightarrow d_{xz,yz}$ transitions to be the highest in energy. As they are coupled to the $d_{x^2-y^2}$ orbital through L_{\pm} , we can exclude their identification as the 0.4 eV peak through the same reasoning given above for d_{xy} . Such an identification would also cause the matrix element [Eq. (1)] for the magnon sidebands to vanish due to the odd symmetry of $d_{xz,yz}$ under $z \rightarrow -z$.

Thus we conclude that the exciton near 0.4 eV most likely results from the transition to the $d_{3z^2-r^2}$ state. It is the only Cu-ion crystal-field level not coupled to $d_{x^2-y^2}$ by L . However, this identification is itself not free of controversy. While cluster calculations [18] predict that the $d_{3z^2-r^2}$ is the lowest energy excited state, they typically give energies in the range 0.9–1.6 eV. For point ion calculations, the crystal-field Hamiltonian can be written in terms of operators that are second and fourth order in the orbital angular momentum operators [19]. To explain the low energy of the $d_{3z^2-r^2}$ state relative to the d_{xy} we must assume that the second-order terms are more effectively screened than the fourth-order ones. At present the low energy for the $d_{x^2-y^2} \rightarrow d_{3z^2-r^2}$ exciton is an open question.

In addition, the similar energy for the $d_{3z^2-r^2}$ exciton in the four materials initially appears surprising because of their differing out-of-plane structure. However, point ion calculations give very similar level spacings for these materials because the primary energy scale is set by the four nearest oxygen ions. The screening is expected to be very similar as well.

The primary unresolved issue is the electric-dipole-allowed nature of the sharp peak near 0.4 eV. Pure $d \rightarrow d$ transitions are dipole forbidden in these materials because of the inversion symmetry of the Cu site; since the ~ 0.4 eV peak is intrinsic we thus conclude that it cannot be the bare exciton. We anticipate that the $d_{x^2-y^2} \rightarrow d_{3z^2-r^2}$ exciton will mix with 2-magnon excitations as they have the same symmetry and comparable energies. According to Tanabe *et al.* [10], the 2-magnon excitation is weakly dipole allowed in orthorhombic La_2CuO_4 because the Cu-O-Cu linkage does not have a center of symmetry; concomitantly it is forbidden in the tetragonal crystals. One might speculate that the low-energy shoulder seen only for La_2CuO_4 results from mixed exciton-2-magnon processes and that the primary peak seen in all four materials is an exciton-magnon [15]

or exciton-phonon bound state which is weakly electric-dipole allowed. Clearly the electric-dipole-allowed nature of the 0.4 eV peak presents a well-posed challenge for theory.

Our discovery of low-energy intrinsic excitations has implications for the doped copper oxides. Since defects break the inversion symmetry we expect the spectral weight for the primary exciton to grow with doping. Furthermore, the addition of holes, which strongly modify the antiferromagnetic ground state, is likely to introduce new matrix elements for dipole-allowed exciton-magnon excitations. For the same reason, it would not be surprising that the sharp features observed here broaden with increasing dopant density. However, the explicit connection between our results in the undoped materials and the ubiquitous mid-infrared absorption band observed in superconductors [20] requires further research.

The authors thank A. Cassanho, B. Keimer, and A. Levy for supplying some of the crystals used in these measurements. We thank S. Girvin, P. Littlewood, A. McMahan, and G. Sawatzki for helpful comments. This work was supported by the National Science Foundation Grants No. DMR 90-07825, No. DMR 90-22933, and No. DMR 90-14839. J.M.G. also acknowledges partial support from the NTT Foundation.

-
- [1] D. B. Tanner and T. Timusk, in *Physical Properties of High-Temperature Superconductors III*, edited by D. Ginsberg (World Scientific, Singapore, 1992).
 - [2] S. Uchida *et al.*, Phys. Rev. B **43**, 7942 (1991).
 - [3] G. A. Thomas, in *Proceedings of the 39th Scottish Universities Summer School in Physics, St. Andrews* (Adam Hilger, New York, 1991).
 - [4] Y. Hidaka *et al.*, J. Cryst. Growth **91**, 463 (1988).
 - [5] J. P. Falck *et al.*, Phys. Rev. Lett. **69**, 1109 (1992).
 - [6] D. Vaknin *et al.*, Phys. Rev. B **41**, 1926 (1990).
 - [7] M. Greven *et al.* (unpublished).
 - [8] L. P. Lee *et al.*, Phys. Rev. B **42**, 2182 (1990).
 - [9] M. L. Jones *et al.*, Phys. Rev. B **46**, 611 (1992).
 - [10] Y. Tanabe *et al.*, Phys. Rev. Lett. **15**, 1023 (1965).
 - [11] J. B. Parkinson, J. Phys. C **2**, 2012 (1969); J. B. Parkinson and R. Loudon, J. Phys. C **1**, 1568 (1968).
 - [12] R. A. Cowley *et al.*, Phys. Rev. Lett. **23**, 86 (1969).
 - [13] K. B. Lyons *et al.*, Phys. Rev. B **39**, 9693 (1989).
 - [14] S. Tajima *et al.*, Physica (Amsterdam) **168C**, 117 (1990).
 - [15] R. S. Meltzer *et al.*, Phys. Rev. Lett. **21**, 913 (1968).
 - [16] J. P. Falck *et al.* (unpublished).
 - [17] R. Liu *et al.* (unpublished).
 - [18] A. K. McMahan *et al.*, Phys. Rev. B **42**, 6268 (1990); A. K. McMahan *et al.*, Phys. Rev. B **38**, 6650 (1988); H. Eskes *et al.*, Phys. Rev. B **41**, 288 (1990); however, see also M. Grilli *et al.*, Phys. Rev. B **42**, 6233 (1990).
 - [19] A. Abragam and B. Bleaney, *Electron Paramagnetic Resonance of Transition Ions* (Clarendon Press, Oxford, 1970), p. 372.
 - [20] H. P. Geserich *et al.*, Europhys. Lett. **6**, 277 (1988).